Molecular Biology of the Cell
Vol. 19, 2003–2013, May 2008

Stathmin Activity Influences Sarcoma Cell Shape, Motility, and Metastatic Potential

Barbara Belletti,*† Milena S. Nicoloso,*†‡ Monica Schiappacassi,* Stefania Berton,* Francesca Lovat,* Katarina Wolf,§‖ Vincenzo Canzonieri,¶ Sara D'Andrea,* Antonella Zucchetto,# Peter Friedl,§‖ Alfonso Colombatti,*@†† and Gustavo Baldassarre*

*Division of Experimental Oncology 2, ¶Division of Pathology, and #Clinical and Experimental Hematology Research Unit, Centro di Riferimento Oncologico, Istituto Nazionale Tumori, IRCCS Aviano 33081, Italy; §Rudolf-Virchow Center, Deutsche Forschungsgemeinschaft Center for Experimental Biomedicine and Department of Dermatology, University of Wuerzburg, 97080 Wuerzburg, Germany; and @Dipartimento di Scienze e Tecnologie Biomediche and ††MATI Center of Excellence, University of Udine, 33100 Udine, Italy

Submitted September 12, 2007; Revised February 13, 2008; Accepted February 15, 2008
Monitoring Editor: Josephine Adams

The balanced activity of microtubule-stabilizing and -destabilizing proteins determines the extent of microtubule dynamics, which is implicated in many cellular processes, including adhesion, migration, and morphology. Among the destabilizing proteins, stathmin is overexpressed in different human malignancies and has been recently linked to the regulation of cell motility. The observation that stathmin was overexpressed in human recurrent and metastatic sarcomas prompted us to investigate stathmin contribution to tumor local invasiveness and distant dissemination. We found that stathmin stimulated cell motility in and through the extracellular matrix (ECM) in vitro and increased the metastatic potential of sarcoma cells in vivo. On contact with the ECM, stathmin was negatively regulated by phosphorylation. Accordingly, a less phosphorylable stathmin point mutant impaired ECM-induced microtubule stabilization and conferred a higher invasive potential, inducing a rounded cell shape coupled with amoeboid-like motility in three-dimensional matrices. Our results indicate that stathmin plays a significant role in tumor metastasis formation, a finding that could lead to exploitation of stathmin as a target of new antimetastatic drugs.

INTRODUCTION

Stathmin 1 (also known as OP18 [OncoProtein 18] or metablastin) is a ubiquitously expressed cytosolic phosphoprotein, enriched in neuronal cells and showing a peak of expression at the end of gestation (Koppel *et al.*, 1990). Like other members of its family (stathmin 2, 3, and 4), stathmin 1 (hereafter stathmin) is a microtubule (MT)-destabilizing protein (Curmi *et al.*, 1999), acting either by promoting MT catastrophe (Belmont and Mitchison, 1996) or by sequestering free $\alpha\beta$-tubulin heterodimers (Howell *et al.*, 1999).

Experimental evidence suggests that stathmin MT-depolymerizing activity is negatively regulated by phosphorylation on four serine (S) residues (S16, S25, S38, and S63). Numerous serine-threonine kinases phosphorylate stathmin in vitro and in living cells (Curmi *et al.*, 1999), supporting the hypothesis that stathmin could act as a relay for multiple signal transduction pathways (Sobel *et al.*, 1989). Studies conducted in vivo in mice (Jin *et al.*, 2004) and *Drosophila* (Ozon *et al.*, 2002; Borghese *et al.*, 2006) and in vitro on cultured cells (Baldassarre *et al.*, 2005; Giampietro *et al.*, 2005; Ng *et al.*, 2006; Watabe-Uchida *et al.*, 2006) demonstrated that stathmin plays a role in several cellular processes, including neuritis formation and cell movement. Moreover, stathmin is overexpressed in several types of human cancers, suggesting that it could have a role in tumor progression (Melhem *et al.*, 1991; Curmi *et al.*, 2000; Price *et al.*, 2000). Recently, a point-mutated stathmin protein (which carries a substitution at Q18) was identified in esophageal cancer. This mutation impairs stathmin phosphorylation, increases its activity, and transforms mouse fibroblasts (Misek *et al.*, 2002).

MT stability influences cell motility in a cell- or context-dependent manner (Etienne-Manneville, 2004), and recent studies found that cell contact with the extracellular matrix (ECM) induces MT stabilization (Etienne-Manneville, 2004; Palazzo *et al.*, 2004), suggesting that cell movement through ECM substrata may also be regulated by the levels and/or activity of the MT-regulating proteins.

Together, these findings support the hypothesis that altering the MT network by deregulation of stathmin could influence cell motility, particularly in cancer cells. In the current study, we addressed this hypothesis by investigating the role of stathmin and its phosphorylation status in regulating cell shape, growth, adhesion, and motility in vitro and in vivo.

This article was published online ahead of print in *MBC in Press* (http://www.molbiolcell.org/cgi/doi/10.1091/mbc.E07–09–0894) on February 27, 2008.

† These authors contributed equally to this work.

Present addresses: ‡ Department of Experimental Therapeutics, The University of Texas M. D. Anderson Cancer Center, Houston, TX; ‖ Department of Cell Biology, NCMLS Radboud University Nijmegen Medical Centre, Nijmegen, The Netherlands.

Address correspondence to: Gustavo Baldassarre (gbaldassarre@cro.it).

MATERIALS AND METHODS

Cell Culture, Transfection, and Treatments

HT-1080 fibrosarcoma cells were grown in DMEM supplemented with 10% fetal bovine serum (FBS; Sigma, St. Louis, MO) and transfected using FuGENE 6 (Roche, Indianapolis, IN). Experiments were performed 48 h after transfection. Stable cell clones were obtained by selecting cells in puromycin (2 μg/ml) or hygromycin (400 μg/ml) for FLAG-tagged or untagged vectors, respectively. All experiments were performed on two independent clones derived from each construct. The expression vectors and the adenovirus used in this study are described in the Supplementary Materials and Methods.

Proliferation, Adhesion and Migration Assays and Time-Lapse Microscopy

Proliferation, adhesion and migration assays, and time-lapse microscopy were performed as previously described (Baldassarre *et al.*, 2005, Wolf *et al.*, 2003) and are extensively described in the Supplementary information.

Immunoblotting, Immunoprecipitation, and Immunofluorescence

Western blot analysis was performed as previously described (Baldassarre *et al.*, 2005). Primary antibodies (Abs) were purchased from Sigma (actin, α-tubulin, acetylated α-tubulin, polyglutamylated-tubulin, and FLAG-M1), Santa Cruz Biotechnology (Santa Cruz, CA; β-tubulin, vinculin, AKT, and FAK), Transduction Laboratories (Lexington, KY; stathmin/metablastin), Roche (enhanced green fluorescent protein [EGFP]), Cell Signaling (Beverly, MA; stathmin, phospho-mitogen-activated protein kinase [pMAPK], pAKT, pFAK, and MAPK) and Chemicon (Temecula, CA; detyrosinated Glu-tubulin). Secondary HRP-conjugated antibodies were from Amersham (Piscataway, NJ); secondary fluorescein isothiocyanate (FITC)-, Texas red– and Alexa Fluor 633–conjugated antibodies were from Jackson ImmunoResearch (West Grove, PA) or Molecular Probes (Eugene, OR). For immunofluorescence staining, cells grown in Matrigel or Collagen I drops on coverslips for the indicated time were fixed in PBS, 4% paraformaldehyde (PFA) at room temperature, permeabilized in PBS, 0.2% Triton X-100, and blocked in PBS, 1% BSA, 10% normal goat serum. Incubation with primary antibodies was performed for 3 h at room temperature (or overnight at 4°C) in PBS, 1% BSA, and 1% normal goat serum. Nuclear staining was performed with 1 μg/ml Hoechst 33258 in PBS for 10 min at room temperature. Stained cells were studied using a confocal laser-scanning microscope (TSP2; Leica, Deerfield, IL) interfaced with a Leica DMIRE2 fluorescent microscope or using a Nikon Diaphot 200 epifluorescent microscope (Melville, NY) equipped with distinguishing filters. Cell area and perimeter were calculated using the Leica LAS software.

Measurement of Soluble or Polymerized Tubulin and Tubulin Dilution Assay

Studies on tubulin polymerization were performed as reported (Baldassarre *et al.*, 2005) and are extensively described in the Supplementary Information.

Tumor Collection and Analysis

All primary and metastatic sarcomas were diagnosed, and samples were collected at the CRO National Cancer Institute of Aviano, Italy. Equal amounts of proteins extracted from 16 malignant fibrohistiocytomas and 23 leiomyosarcomas and their normal peritumoral tissues were analyzed for stathmin and actin expression. Expression of stathmin was quantified by densitometric scanning of the blots and normalized against actin. Immunohistochemical study of stathmin expression in primary and metastatic sarcomas was performed using a commercial anti-stathmin Ab (Cell Signaling). To unmask the antigens from paraffin, samples were heated in the microwave for 30 min at 250 W in citrate buffer at pH 7.8.

RNA Extraction and RT-PCR

RNA from normal and neoplastic specimens from mouse organs and xenografts was extracted using the RNeasy kit (Qiagen, Chatsworth, CA). One microgram of total RNA was retrotranscripted using MuVL Reverse Transcriptase and random examers (Promega, Madison, WI); 1/10 of the obtained cDNAs were then amplified using primers for the human stathmin sequence, to amplify the region between amino acids 1-99 (Baldassarre *et al.*, 2005) or with primers for human GAPDH mRNA.

In Vivo Experiments

Nude mice were injected subcutaneously with 1×10^6 HT-1080 parental (n = 4), clone vector 1 (n = 4), stathmin^{WT} clone A3 (n = 6), stathmin^{Q18E} clones B9 (n = 4), or F7 (n = 4) cells, and tumor growth was monitored for 20 d. Mice were then killed to analyze xenografts, blood, liver, lung, and spleen for the presence of HT-1080 cells, using RT-PCR with primers specific for the transfected vectors (pFLAG for A3 and B9 or pcDNA3.1 for V1 and F7). For local invasion, 5×10^5 parental (n = 4) and stathmin^{Q18E} B9 (n = 4) HT-1080 cells were included in Matrigel, injected subcutaneously in nude mice, and allowed to grow for 15 d. Tumors were then excised along with the surrounding mouse tissue and analyzed by H&E staining. For lung metastasis formation, 5×10^5 vector 1 (n = 4) or stathmin^{Q18E} F7 (n = 4) HT-1080 cells were injected in the mouse tail vein, and lungs were analyzed 30 d later by H&E staining. For the quantification of lung metastasis, 10 sections per lung were analyzed. For small interfering RNA (siRNA) experiments, HT-1080 cells were infected (MOI 300) with adenovirus (Ad)-Cont siRNA (control) or Ad-stathmin siRNA; 3 d later, the cells (5×10^5) were injected into nude mice (n = 4). After 15 d, intratumoral injection of Ads was repeated, and the mice were killed on day 30 from the initial injection.

RESULTS

Stathmin Is Deregulated in Human Sarcoma

Stathmin is overexpressed in many tumor types (e.g., leukemias, breast cancer, hepatocellular carcinoma), but its contribution to tumorigenesis is still poorly understood. Sarcomas are a class of mesenchymal tumors characterized by an important invasive potential, responsible for their high rate of local recurrence after surgery and distant metastasis. To determine the role of stathmin in tumorigenesis, we evaluated its expression levels, using Western blot (Figure 1) and immunohistochemistry (Supplementary Figure 1, A–D), in a panel of human sarcomas (16 malignant fibrohistiocytomas and 23 leiomyosarcomas) and the normal tumor-free surrounding tissue. More than 80% of the cases displayed overexpression of stathmin in tumor specimens compared with adjacent normal tissue (Figure 1A), with an average value for the stathmin/actin ratio (n = 10) that was twofold higher, although this difference was not statistically significant ($p = 0.187$, Student's t test; Figure 1C). When tumors were sorted as primary or recurrent/metastatic, stathmin expression was strongly associated with tumor relapse and distant metastasis formation (Figure 1, B and C). Recurrent (n = 15) and metastatic sarcomas (n = 14) displayed a stathmin/actin ratio ~20-fold higher than that of the normal tissue, with the difference being highly significant ($p = 0.001$ and 0.0005, respectively). Furthermore, stathmin expression was greatly increased ($p = 0.002$) between primary and recurrent/metastatic sarcomas, suggesting a role in tumor progression. Because stathmin's biological functions are negatively regulated by phosphorylation, we also checked whether stathmin overexpression was paralleled by a variation in its phosphorylation status. Focusing on normal and sarcoma samples expressing comparable levels of total protein, we found a reduction of S16 phosphorylation in neoplastic samples compared with normal ones (Supplementary Figure 1F). Similar conclusions were drawn by studying stathmin phosphorylation in seven cases of patients with recurrent diseases (Figure 1D). The expression of pS16, total stathmin, and their ratios were evaluated by Western blot and densitometric scanning of the blots. As shown in Figure 1D recurrent diseases showed a decreased pS16/stathmin ratio (4/7 cases) or a de novo expression of total stathmin protein (two cases). These findings support the hypothesis that an increased stathmin expression coupled with an increase in its activity could be relevant in the process of local invasion and distant dissemination.

Stathmin Stimulates Cell Motility by Destabilizing MTs

To get deeper insight into the molecular mechanism through which stathmin contributes to sarcoma invasiveness, we tested the in vitro ability of stathmin to drive fibrosarcoma cell motility. Having previously demonstrated that p27^{kip1} overexpression reduces ECM-dependent cell motility by inhibition of stathmin tubulin-sequestering activity (Baldassarre *et al.*, 2005), we better characterized the role of stathmin in cell motility by separating its tubulin-sequestering activ-

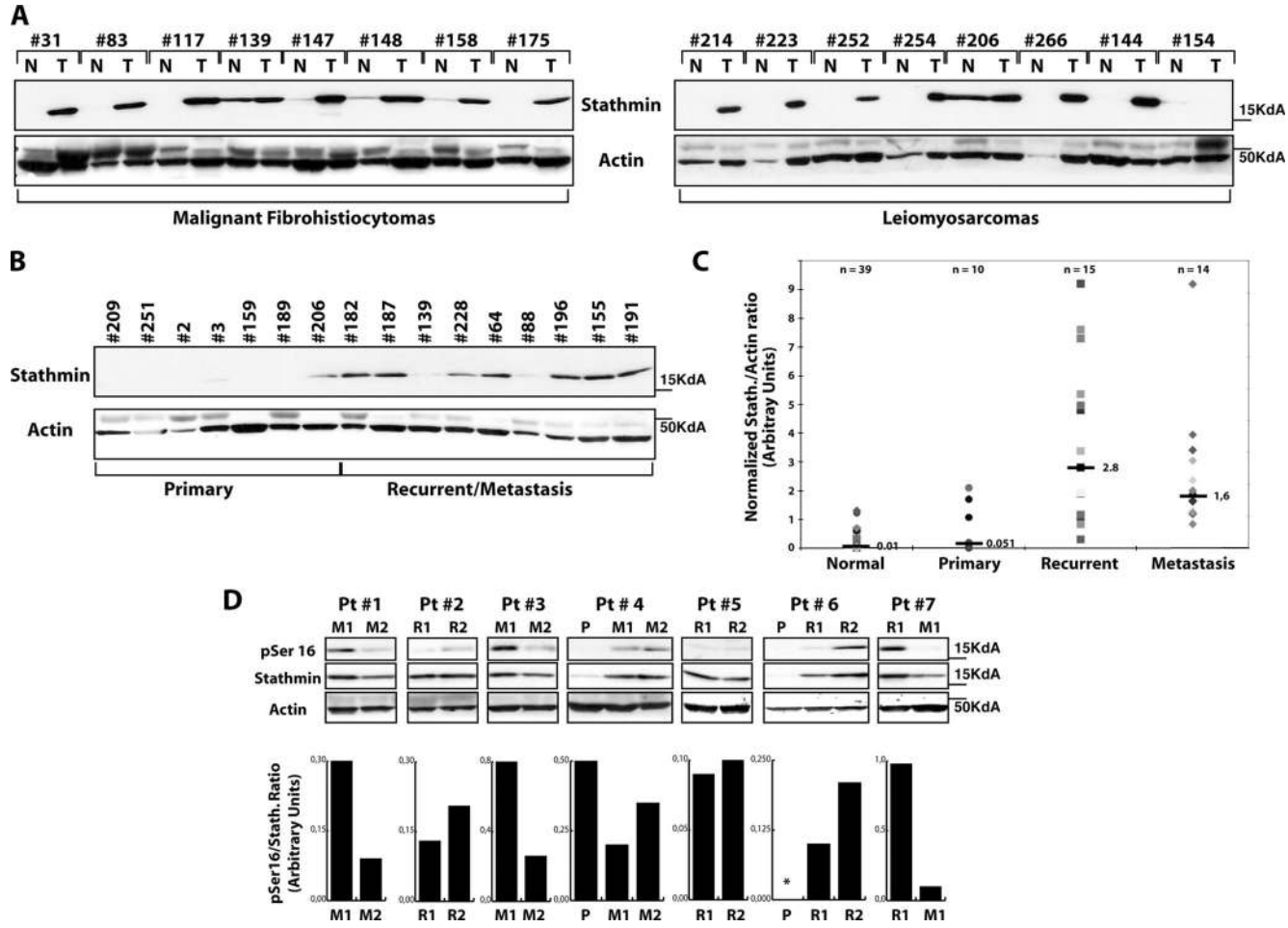

Figure 1. Stathmin is overexpressed in recurrent and metastatic sarcomas. (A) Western blot analysis of stathmin expression in malignant fibrohistiocytomas (T, left panels) or leiomyosarcomas (T, right panels) and their paired normal (N) tissues. Actin expression was used as normalization control. (B) Western blot analysis of stathmin and actin expression in primary and recurrent/metastatic sarcomas. (C) Statistical analysis of the stathmin/actin ratio in normal, primary, recurrent, and metastatic sarcoma samples, evaluated by densitometric scanning of the Western blots. The median ratio for each group is reported. (D) pS16 and total stathmin expression in seven patients (Pt) with relapsed local (R) or metastatic (M) diseases. Actin expression was used as normalization control. The ratio between pS16 and stathmin expression, evaluated by densitometric scanning of the blots, is illustrated in the bottom graphs. P, primary sarcoma; *not detectable.

ity from its catastrophe-promoting one. To this purpose, we performed an ECM-dependent motility assay utilizing stathmin^{WT} and two deletion mutants: stathmin$^{1-99}$, retaining the catastrophe-promoting activity, and stathmin$^{25-149}$, retaining the tubulin-sequestering activity (Howell *et al.*, 1999). In a human fibrosarcoma cell line (HT-1080), stathmin^{WT} overexpression greatly enhanced cell migration through a fibronectin (FN)-coated Transwell. The stathmin$^{25-149}$ tubulin-sequestering mutant induced a similar effect, whereas stathmin$^{1-99}$ was unable to do so (Figure 2A), indicating that stathmin tubulin-sequestering activity is sufficient to stimulate cell motility on ECM substrata. Given the fact that stathmin is a MT-destabilizing protein and that MT dynamics play a central role in cell motility, we investigated whether the expression of these stathmin mutants was accompanied by differences in the cellular MT stability. Stable MTs, i.e., MTs with a half-life longer than 15 min (Verhey and Gaertig, 2007), can be distinguished by a variety of posttranslational modifications (Khawaja *et al.*, 1988; Verhey and Gaertig, 2007), such as acetylation, poly-glutamylation, and detyrosination, all recognizable with specific antibodies. We explored the amount of stable MTs in HT-1080 cells overexpressing stathmin^{WT} or the deletion mutants after 60 min of FN adhesion, by immunofluorescence and Western blot analysis. Expression of EGFP-stathmin^{WT} and EGFP-stathmin$^{25-149}$ proteins dramatically decreased the amount of cellular acetylated/stable MTs (Figure 2C, left and middle panels), whereas the EGFP-stathmin$^{1-99}$ mutant has only minor effects (right panels). Consistently, differential extraction of soluble and polymerized tubulin fractions followed by Western blot analysis also confirmed that the stathmin$^{1-99}$ mutant displayed a compromised ability to destabilize MTs after cell adhesion to the ECM (Figure 2B).

Collectively, these data support a role for stathmin in ECM-driven cell migration that is achieved through the MT-destabilizing activity of its tubulin-sequestering domain.

Stathmin Is Phosphorylated after Cell Adhesion to ECM Substrata

Stathmin tubulin-sequestering activity is controlled by serine phosphorylation (Curmi *et al.*, 1999) and by association with several proteins, such as p27^{kip1} (Baldassarre *et al.*, 2005) or STAT3 (Ng *et al.*, 2006). In both cases, these interactions translated into an alteration of cell motility. We

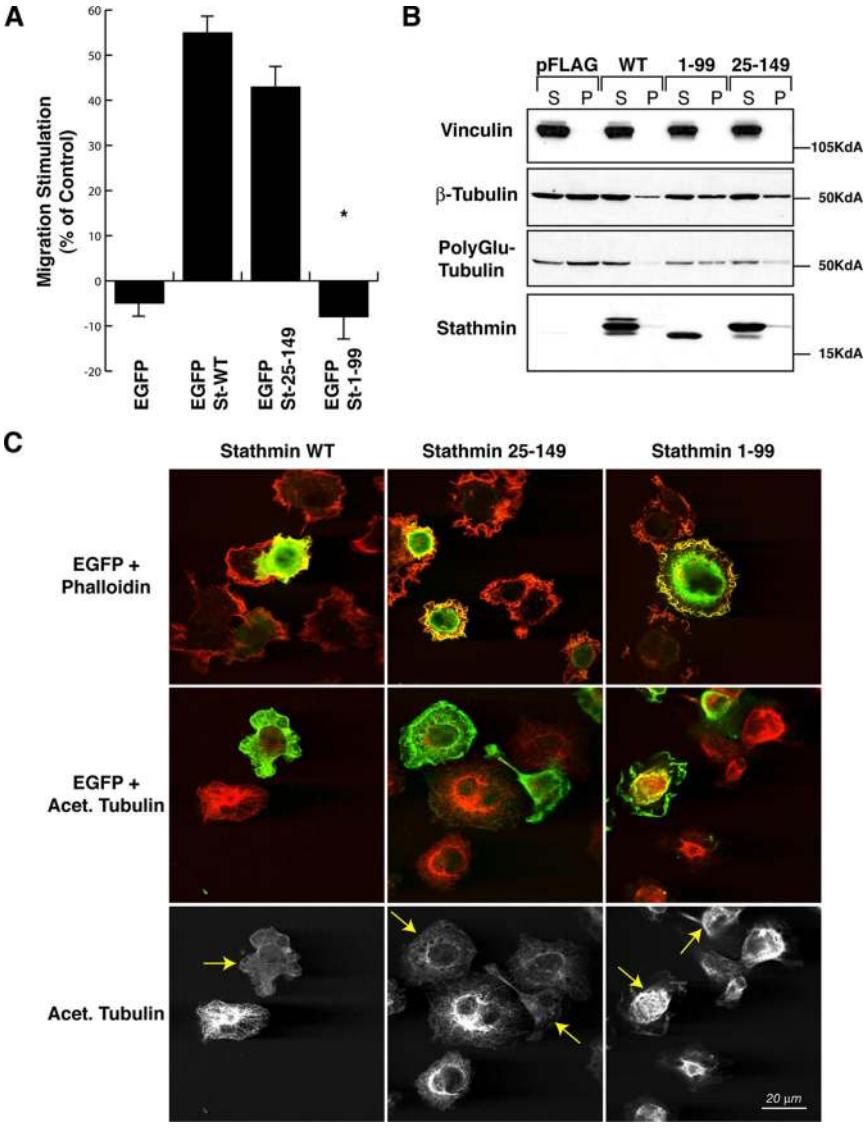

Figure 2. Stathmin tubulin-sequestering activity is necessary to stimulate cell motility. (A) Migration through FN-coated FluoroBloks of HT-1080 cells transiently transfected with the indicated EGFP vectors. Data are expressed as the percentage of stimulation with respect to the surrounding untransfected cells and represent the mean (±SD) of three independent experiments, in which at least 100 transfected cells were counted. (B) Western blot analysis of soluble (S) and polymerized (P) fractions of tubulin in HT-1080 cells transiently transfected with the indicated pFLAG-vectors and adhered to FN for 60 min. The expression of vinculin (loading control), β-tubulin, polyglutamylated-tubulin, and stathmin is shown. (C) Confocal images of HT-1080 cells transiently transfected with the indicated EGFP constructs (green) and stained with phalloidin or acetylated tubulin (red). In the bottom panels, only the acetylated tubulin staining is shown. Yellow arrows indicate the transfected cells.

therefore sought to investigate whether stathmin phosphorylation as well was implicated in the regulation of ECM-driven cell motility.

We first analyzed the effect of cell–ECM contact on stathmin phosphorylation in serum-starved HT-1080 cells allowed to adhere to FN for up to 90 min. Using three phosphospecific antibodies recognizing pS16, pS25, and pS38 of stathmin (Gavet *et al.*, 1998), we observed an obvious increase of phosphorylated stathmin at S16 and S38 after 60 min of adhesion to FN (Figure 3, A and B). Endogenous pS25 was not detectable, and total stathmin levels were not affected by cell adhesion under these conditions (Figure 3B). Time-course analysis of cells transiently transfected with a FLAG-tagged stathmin vector confirmed that phosphorylation of S16, S38, and also S25 increased significantly after 30–90 min of adhesion, when FN (Figure 3C) and collagen I (Coll I; Supplementary Figure 5B and data not shown) were used as substrata.

To test whether these phosphorylations had any effect on stathmin promigratory activity, we generated a less phosphorylable stathmin mutant carrying the Q18E substitution. The stathmin^{Q18E} mutant was originally identified in human cancers (Misek *et al.*, 2002) and was shown to have impaired phosphorylation on S16 (and partially on S25 and S38), to increase MT-depolymerization activity and to induce cell transformation (Misek *et al.*, 2002). We therefore chose to use this more "physiological" mutant for our experiments, rather than the "classical" serine-alanine substitution mutants. Transiently transfected HT-1080 cells were serum starved and then adhered to FN for 60 min. Under these conditions, a marked reduction of S16 phosphorylation was observed in stathmin^{Q18E}-expressing cells, compared with stathmin^{WT}, whereas no significant difference in the levels of pS25 and pS38 was found (Figure 3C). Similar results were obtained by immunofluorescence analysis of both endogenous and ectopically transfected stathmin in HT-1080 cells adhered to FN (Figure 3D and Supplementary Figure 2). These experiments highlight an FN-dependent signaling pathway leading to stathmin phosphorylation and to the regulation of its MT-destabilizing properties. Additional experiments will be required to identify the specific kinase(s) participating in this pathway that leads to the ECM-driven regulation of stathmin.

Generation and Characterization of Stathmin Stable Cell Clones

Several stable HT-1080 cell clones overexpressing the stathmin^{WT} or stathmin^{Q18E} proteins were generated using either

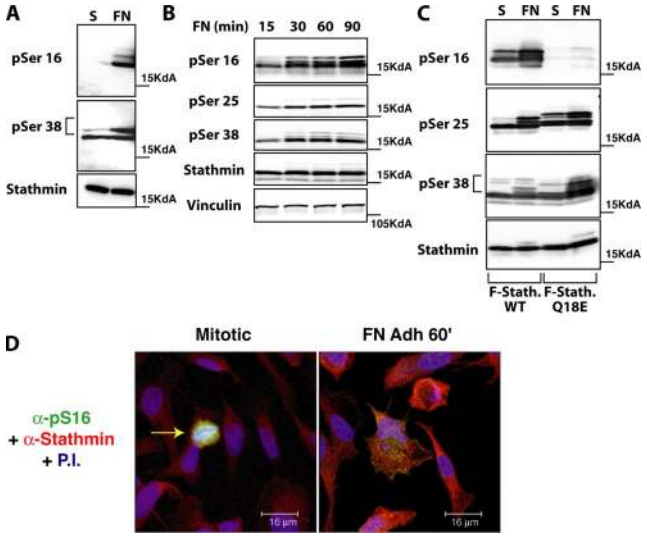

Figure 3. Stathmin is phosphorylated in an adhesion-dependent manner. (A) Expression of endogenous stathmin pS16 and pS38 in HT-1080 cells, serum starved for 8 h (S) or adherent to FN for 60 min (FN). (B) Expression of stathmin pS16, pS25, and pS38 in HT-1080 cells, transiently transfected with pFLAG-stathmin, serum starved for 8 h, and adhered to FN for the indicated times. Vinculin expression was used as loading control. (C) Expression of pS16, pS25, and pS38-stathmin in HT-1080 cells, transiently transfected with FLAG-stathmin^{WT} or FLAG-stathmin^{Q18E}, serum starved for 8 h (S), or adhered to FN for 60 min (FN). (D) Endogenous stathmin is phosphorylated on S16 in an adhesion-dependent manner. S16 phosphorylation was detected using the phosphospecific Ab against pS16 and a secondary FITC-conjugated anti-rabbit Ab pseudocolored in green; total stathmin expression was detected using a monoclonal Ab against human stathmin (Transduction Laboratories) and a secondary anti-mouse AlexaFluor 633-conjugated Ab and pseudocolored in red; nuclei were detected using propidium iodide and pseudocolored in blue. In the left panel, the pS16 stathmin phosphorylation is specifically detected in a mitotic cell (yellow arrow). In the right panel, the S16 phosphorylation of the endogenous stathmin upon cell adhesion to FN for 60 min is shown. Yellow color indicates the colocalization of green and red fluorescence.

untagged or FLAG-tagged constructs. The complete characterization in terms of proliferation, survival, and adhesion ability of HT-1080 clone V1 (transfected with the empty vector) and four different stathmin-expressing clones used in this work is extensively described in the Supplementary information. Importantly, we observed that stable stathmin overexpression in HT-1080 cells did not significantly modify cell proliferation, survival, or adhesion properties (Supplementary Figures 3–5). Thus, we continued to focus our attention on the role of stathmin in cell motility.

Stathmin Expression Enhances 3D Migration and Invasion

Parental HT-1080 and stathmin-expressing clones were tested in different types of ECM-driven migration assays, using FN- or Matrigel-coated Transwells or ECM inclusions. Both stathmin^{WT} and stathmin^{Q18E} proteins promoted cell migration (Figure 4A), invasion (Figure 4B), and evasion (Figure 4C) through and from ECM substrata, with stathmin^{Q18E} slightly more active than stathmin^{WT} in all types of assays. To exclude the possibility that clonal selection could be responsible, at least partially, for the promigratory behavior of stathmin-expressing cells, transiently transfected cells were also used. One day after transfection, cells were plated on top of or below a 1-mm-thick Matrigel layer and allowed to invade the matrix for 3 days. The extent of Matrigel invasion, as evaluated by confocal microscopy, demonstrated that overexpression of EGFP-stathmin^{WT} increased the ability of HT-1080 cells to invade Matrigel and that the Q18E substitution further amplified this invasive potential (Figure 4D). Consistently, down-regulation of endogenous stathmin, by means of an adenovirus (Ad) expressing stathmin siRNA, decreased HT-1080 cell migration through FN-coated Transwells (Figure 4E). The concomitant expression of either EGFP-stathmin^{WT} or EGFP-stathmin^{Q18E} proteins was able to rescue cell migratory ability (Figure 4, F and G). On the whole, these experiments substantiate stathmin involvement in different types of ECM-driven cell motility and the possibility that an altered stathmin phosphorylation pattern, as found in human sarcoma samples (Figure 1F) or in esophageal carcinomas with the Q18E mutation (Misek *et al.*, 2002), increases its promigratory activity.

Stathmin Expression Does Not Enhance Fibrosarcoma Cell Motility in Two-dimensional Assays

Altered MT dynamics have been suggested to exert an inhibitory role on cell motility (Liao *et al.*, 1995; Wittmann *et al.*, 2004). In accordance with this hypothesis, the hyperactivity of stathmin in STAT3-null fibroblasts has been considered the cause of a decreased wound closure (Ng *et al.*, 2006). Importantly, most of these studies were based on two-dimensional (2D) assays, such as wound healing (reviewed in Small *et al.*, 2002; Rodriguez *et al.*, 2003), which substantially differ from motility in 3D matrices or in vivo (Friedl and Brocker, 2000). We thus speculated that stathmin could differently affect cell motility, depending on the type of motility assayed. To verify this hypothesis, HT-1080 clones were tested in 2D experiments. Clones expressing stathmin^{WT} or stathmin^{Q18E} migrated in a manner similar to that of control cells in a wound-healing assay (Figure 5, A and B), demonstrating that stathmin does not substantially affect fibrosarcoma cell directional motility in 2D, as reported by Ng *et al.* (2006) for normal fibroblasts. Using time-lapse microscopy to analyze cell motility under 2D or 3D conditions (Supplementary Movies 1–3), we observed that although in wound healing and in 2D random motility on plastic control and stathmin^{Q18E}-expressing cells designed very similar trajectories, in 3D Collagen I stathmin^{Q18E} cells covered significantly longer distances than control cells did (Figure 5, C–E). Accordingly, stathmin^{Q18E} did not enhance HT-single cell velocities in wound healing (Figure 3F) and in 2D random motility assays (data not shown), whereas in 3D assays stathmin^{Q18E} cells moved significantly faster (Figure 3G).

Stathmin Expression Influences Adhesion-dependent MT Polymerization

To determine whether increased motility of stathmin^{Q18E}-expressing clones corresponded to molecular variations in MT organization, we analyzed the extent of polymerized tubulin in stathmin^{WT} and stathmin^{Q18E} HT-1080 clones, in suspension and after 1 h of adhesion to FN. Western blot analysis of soluble and polymerized protein fractions showed that adhesion to ECM components leads to an important tubulin reorganization, which was in part counteracted when stathmin was not phosphorylable (Figure 6A), confirming that stathmin^{Q18E} has an enhanced capability to interfere with adhesion-dependent MT polymerization. Moreover, after adhesion stathmin^{Q18E} induced a marked reduction in the amount of polymerized MTs, compared with control cells, accompanied by a reduced level of tubulin posttranslational modifications, which are markers of MT

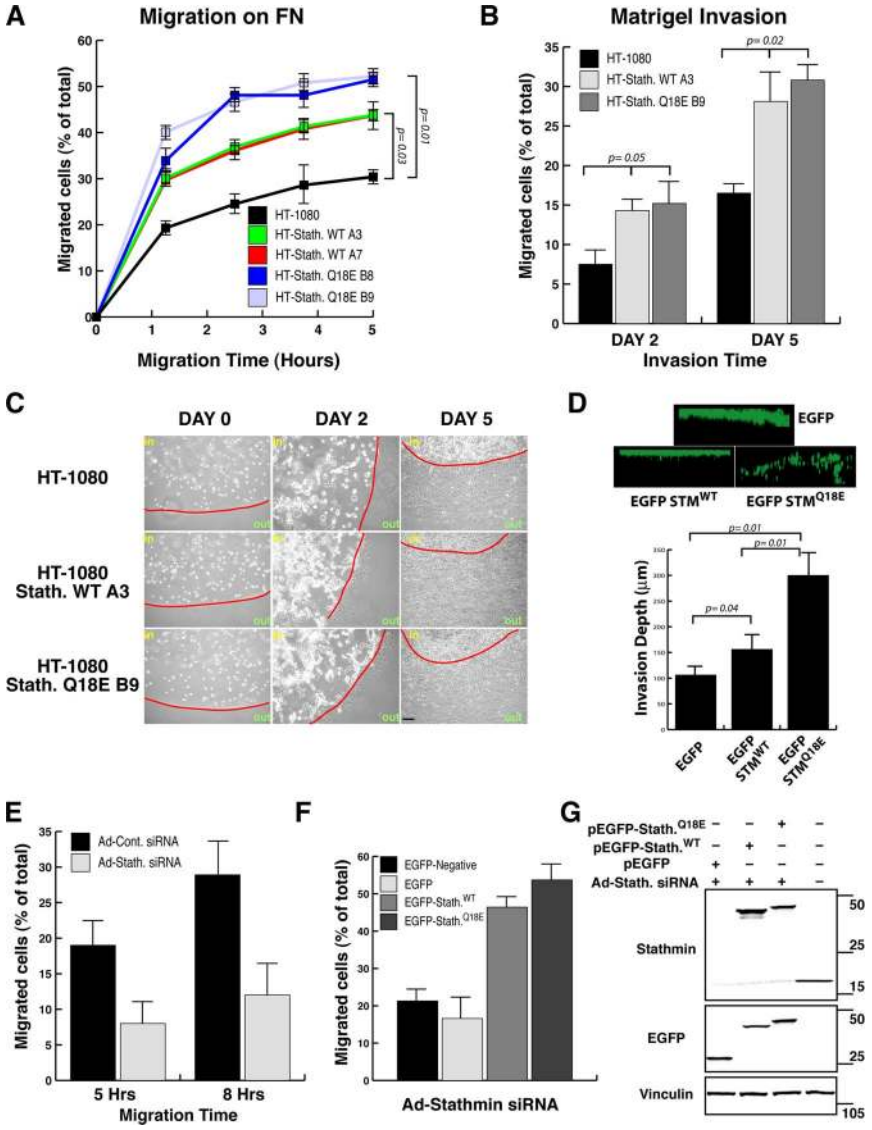

Figure 4. Stathmin^{WT} and stathmin^{Q18E} in HT-1080 cells confer a migratory advantage in ECM-mediated motility assays. (A) Migration of HT-1080 cell clones through FN-coated FluoroBloks, expressed as a function of time. Data represent the mean (±SD) of three independent experiments, performed in duplicate. (B) Invasion of HT-1080 cell clones through Matrigel-coated FluoroBloks, expressed as a function of time. Data represent the mean (±SD) of three independent experiments, performed in duplicate. (C) Matrigel evasion assay. HT-1080 cell clones were included in a Matrigel drop and allowed to evade for 5 d. A typical image from two independent experiments performed in quintuplicate is shown. The red line indicates the border of Matrigel drops. Bar, 100 μm. (D) Invasion depth expressed in micrometers, evaluated by confocal microscopy and representing the mean (±SD) of three independent experiments. Only cells detached from the basal layer were considered as invading cells. Significance was calculated using Student's *t* test. The top images show a typical computer reconstruction of HT-1080 cells, transiently transfected with the indicated EGFP vectors, invading a thick layer of Matrigel. Cells were plated on top of the Matrigel layer and allowed to invade in the presence of NIH-3T3 fibroblast-conditioned medium for 3 d. (E) Migration through FN-coated FluoroBloks of HT-1080 cells infected with the indicated Ads, expressed as a function of time. Data represent the mean (±SD) of two independent experiments, performed in duplicate. (F) Migration through FN-coated FluoroBloks of HT-1080 cells infected with Ad-stathmin siRNA at MOI 300 and then transfected with the indicated EGFP vectors. Percentage of EGFP-negative and -positive migrated cells is reported. Data represent the mean (±SD) of two independent experiments, performed in duplicate. (G) Western blot analysis of endogenous (stathmin) or ectopic (EGFP) stathmin expression in HT-1080 cells, infected with Ad-stathmin siRNA and then transfected with the indicated EGFP vectors. Vinculin expression was used as loading control.

stability (Figure 6B). Interference with adhesion-dependent MT polymerization by both stathmin^{WT} and stathmin^{Q18E} was also demonstrated on transiently transfected HT-1080 cells by Western blot analysis of modified tubulin in polymerized and soluble cellular fractions (Figure 6C). As expected, both endogenous and transfected stathmin resided in the soluble fraction, and stathmin^{Q18E}-expressing cells displayed a reduced phosphorylation of S16 but not of S38 (Figure 6C). Likely for the high levels of transiently expressed stathmin proteins in these experiments, only small differences were noticed between stathmin^{WT} and stathmin^{Q18E} on MT polymerization (Figure 6C, fourth panel). The decrease in MT stability induced by stathmin^{Q18E} was further confirmed by performing the tubulin dilution assay on cells adhered to FN for 1 h and subsequently fixed and stained with an anti-α-tubulin antibody. This assay allows visualization of only stable MTs with a half-life longer than 15 min (Khawaja *et al.*, 1988). Results clearly show that HT-1080 V1 cells retain a threefold higher amount of stable MTs compared with stathmin^{Q18E}-expressing cells (Figure 6D and data not shown). Importantly, immunofluorescence analysis of acetylated (Figure 6E) and detyrosinated tubulin (data not shown) on the same cells cultured on plastic in 2D did not show any significant difference in the content of stable MTs, supporting the hypothesis that stathmin affects MT polymerization after contact with the ECM and that stathmin ECM-dependent phosphorylation controls this activity.

Stathmin Activity Influences HT-1080 Cell Morphology in a 3D Matrix

Different types of cell motility in 3D assays or in vivo have been linked to distinct molecular mechanisms controlling cell morphology (Friedl and Wolf, 2003; Sahai and Marshall, 2003; Wolf *et al.*, 2003). We thus examined the morphology of HT-1080 cell clones up to 24 h after inclusion in 3D matrices in complete or serum-reduced (1% FBS) medium. The shape factor parameter ($4\pi A/P^2$, where A is the cell area and P the cell perimeter), which varies from 0 to 1 for elongated to more circular shapes, respectively (Peris *et al.*, 2006), was used to quantify cell morphology differences. Both in Coll I after 6 h (Figure 7A) and 24 h (Figure 7B) of inclusion and in Matrigel after 24 h (Supplementary Figure 6A), stathmin^{Q18E}-expressing clones (i.e., B9, F7) presented a more rounded morphology, defined by a high shape factor (Figure 7C at 24 h and Supplementary Figure 6, C and E, at 6 h; $p < 0.0001$, Student's *t* test), compared with the elongated morphology

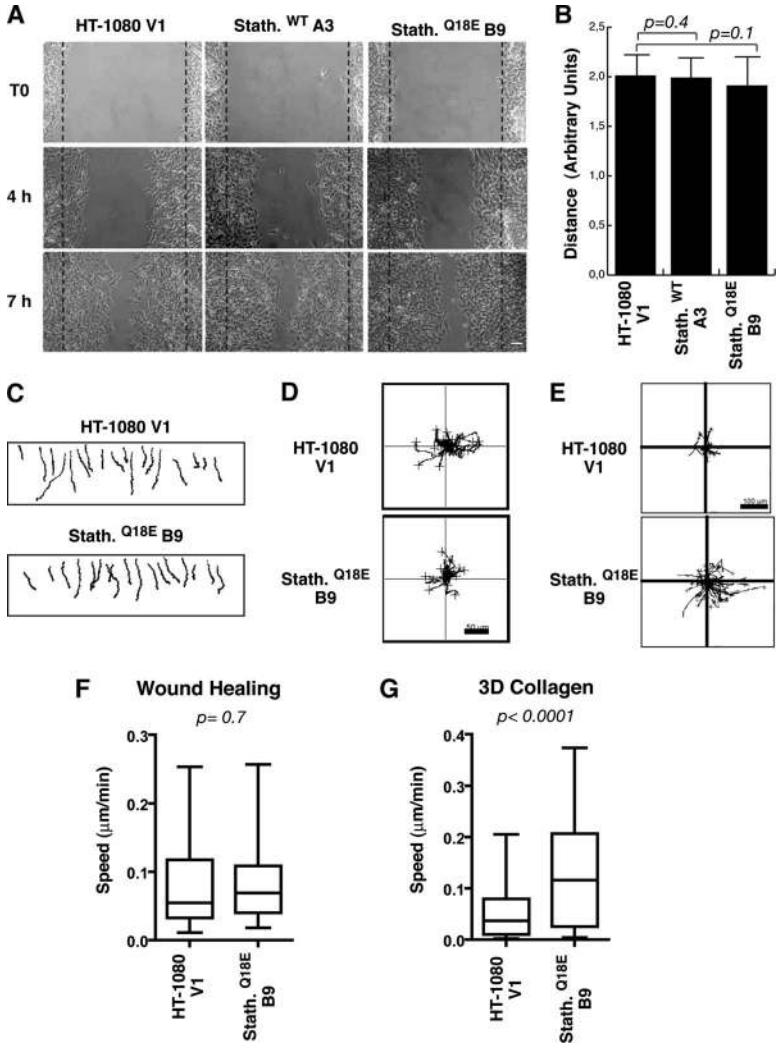

Figure 5. Stathmin expression exerts different effects on HT-1080 cells motility in 2D and 3D assays. (A) Typical images of HT-1080 V1, stathmin^{WT} A3, and stathmin^{Q18E} B9 clones during a wound-healing assay, in which the scratch was performed with a yellow tip. Bar, 100 μm. (B) Quantification of the migration distance covered by HT-1080 V1, stathmin^{WT} A3, and stathmin^{Q18E} B9 clones, over a 24-h period. (C–E) Orthotopically projected cell paths of HT-1080 cell clones, V1 (empty vector), and stathmin^{Q18E} clone B9, allowed to move toward a wound (C), randomly as sparse cells in 2D (D) or immersed in a 3D Coll I matrix (E), in serum-free medium. (F and G) Statistical evaluation (Mann-Whitney U test) of cell speed from experiments described in C and E. Median speeds were 0.07 and 0.09 μm/min for HT-1080 V1 and stathmin^{Q18E} B9, respectively, in the wound-healing assay ($p = 0.7$, Mann-Whitney U test) and 0.03 and 0.11 μm/min for HT-1080 V1 and stathmin^{Q18E} B9, respectively, in the 3D Coll I assay ($p < 0.0001$, Mann-Whitney U test).

of control cells and stathmin^{WT} clones (i.e., vector clone 1 and clone A3, respectively). The absence of an effect on 3D cell morphology of stathmin^{WT} is consistent with the reduced ability of low WT protein levels to interfere with adhesion-dependent MT modification (Figure 6A). Conversely, when cells were simply plated on a plastic dish, no change in cell shape was observed (by shape cell factor calculation and immunofluorescence analysis) between control and stathmin^{Q18E}-expressing cells (Supplementary Figure 7, C and D), in accord with the data obtained with immunofluorescence analysis (Figure 6E). The rounded shape observed in stathmin^{Q18E}-expressing cells in 3D matrices was associated with a decrease in acetylated MTs, as demonstrated by immunofluorescence analysis (Figure 7, D and E, $p < 0.0001$ between control and stathmin Q18E clones) and with a marked reduction of long-lived MTs (Figure 7F), as demonstrated by the tubulin dilution assay. Collectively, our results indicate that stathmin is able to affect cell morphology in a 3D environment by acting on MT stability.

Stathmin Expression Enhances the Metastatic Phenotype of HT-1080 Cells

To verify whether stathmin effects on cell motility observed in vitro could be recapitulated in vivo, nude mice were subcutaneously injected with 1×10^6 parental HT-1080 cells or HT-1080 V1 ($n = 8$), stathmin^{WT} A3 ($n = 6$), and stathmin^{Q18E} B9 or F7 stable cell clones ($n = 8$). After 20 d, mice were killed, and the growth and metastatic ability of each cell clone were evaluated. The analysis of the explanted tumor masses revealed that the local tumor growth was not markedly influenced by stathmin overexpression (Figure 8A). Distant localization of tumor cells was evaluated by RT-PCR on RNA extracted from blood, lung, liver, or spleen, using vector-specific primers (Figure 8, B and C). As shown in Figure 8, B and C, tumor cells were found in distant organs and in the blood of seven of eight mice injected with HT-1080 stathmin^{Q18E} compared with only two of six mice injected with HT-1080 stathmin^{WT} and none of six mice injected with control HT-1080 cells. Stathmin effects on local cell invasion were evaluated instead by subcutaneously injecting into mice ($n = 4$/clone) parental HT-1080 or stathmin^{Q18E} B9 cells previously included in Matrigel. After 15 d, mice were killed and the tumor borders were examined. Although parental HT-1080 cells grew within the Matrigel borders, with only few cells invading the surrounding tissues, cells stably expressing stathmin^{Q18E} aggressively invaded the surrounding host muscular tissues (Figure 8D). We also tested the ability of stathmin^{Q18E}-expressing cells to extravasate and localize to distant organs, in particular to

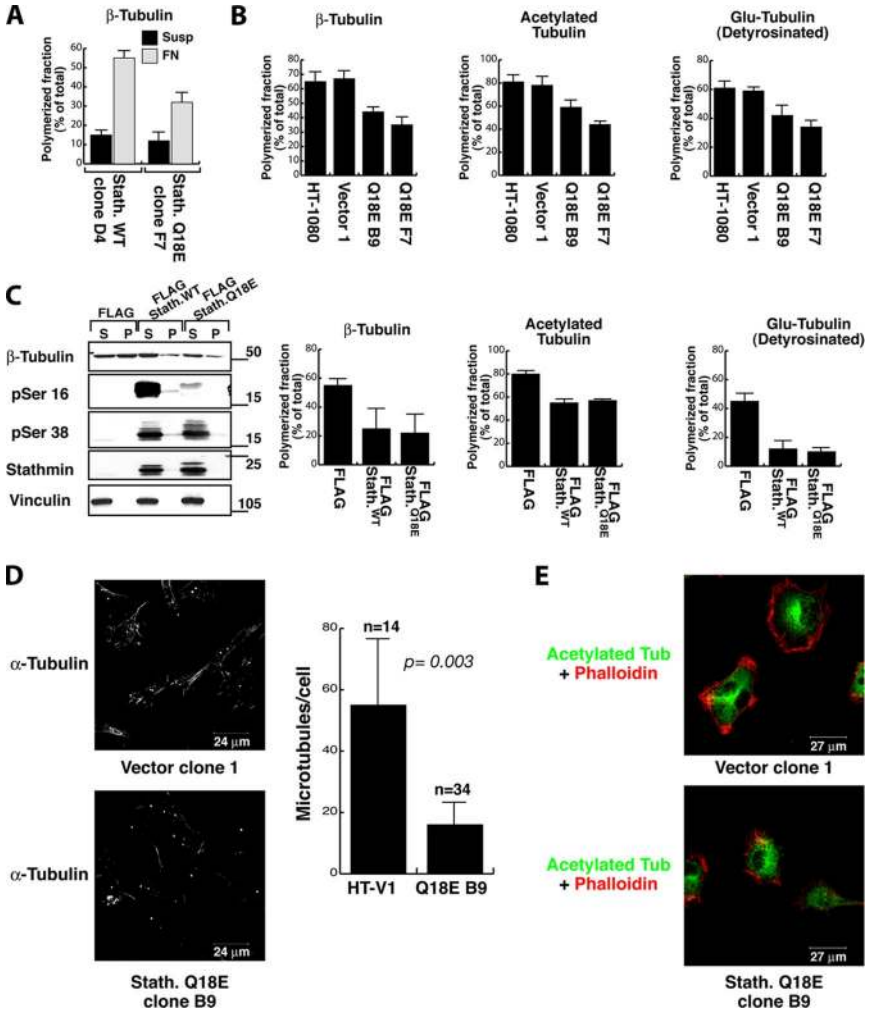

Figure 6. Stathmin expression alters adhesion-dependent MT stabilization in HT-1080 cells. (A) Quantification of the polymerized fraction of β-tubulin in HT-1080 stathmin^{WT} clone D4 and stathmin^{Q18E} clone F7, harvested in suspension (Susp) or after adhesion to FN for 2 h (FN) and analyzed for their soluble (S) or polymerized (P) protein fractions. (B) Percentage of polymerized fractions of β-tubulin, acetylated-tubulin, and detyrosinated (Glu-tub) tubulin, in HT-1080 clone V1 and stathmin^{Q18E} clones B9 and F7, adhered to FN for 60 min. Data determined by densitometric scanning of the blots represents the means (±SD) of three independent experiments. (C) Western blot analysis of HT-1080 cells transiently transfected with pFLAG, pFLAG-stathmin^{WT}, and pFLAG-stathmin^{Q18E} vectors, adhered to FN for 60 min and analyzed for their soluble (S) or polymerized (P) protein fractions. The expressions of β-tubulin, pS16-, pS38, pan-stathmin, and vinculin are shown. Quantification of the polymerized fraction of the indicated cytoskeleton proteins determined by densitometric scanning of the blots is shown in the graphs and represents the mean (±SD) of three independent experiments. (D) Typical images of HT-1080 V1 and stathmin^{Q18E} B9 cell clones, adhered to FN for 1 h, subjected to the tubulin dilution assay and stained with anti-α-tubulin FITC-conjugated Ab. In the graph, the quantification of detectable MTs per cell, representing the mean of two independent experiments, is reported. Data are expressed as percent of MT number with respect to control cells; n represents the number of analyzed cells. (E) Immunofluorescence analysis of acetylated-tubulin (green) expression in HT-1080 clone V1 and stathmin^{Q18E} clone B9 grown on plastic dishes. Phalloidin staining of the same cells is shown in red.

the lungs. To this aim, we injected HT-1080 clone V1 or stathmin^{Q18E} clone F7 cells in the tail vein of nude mice (n = 4/clone); 30 d later, we examined the mouse lungs for the presence of metastases (Figure 8E). Pathological analysis demonstrated that stathmin^{Q18E}-expressing cells (clone F7) readily colonized the lungs, whereas HT-1080 V1 cells did not. When we looked at the levels of polymerized acetylated tubulin in explanted tumor lysates, we observed that they correlated with the metastatic potential of sarcoma cells, because polymerized MTs were strongly diminished in tumors derived from the stathmin^{Q18E}-expressing cells (Figure 8F). The results of the in vivo experiments prove that stathmin^{Q18E} expression strongly increases the metastatic potential of HT-1080 cells, thus substantiating all the in vitro data from motility evasion/invasion assays (Figure 4). Together, the data reported here reinforce the hypothesis that the invasive phenotype of stathmin-expressing cells could be directly related to its activity on MTs and suggest that indeed altered MT stability could also play a role in cell invasiveness in vivo.

DISCUSSION

The present work investigates the role of the MT-destabilizing protein stathmin in sarcoma cell growth and motility and highlights several new aspects regarding the role and regulation of stathmin in human tumorigenesis and the formation of metastases.

Our data point to the tubulin-sequestering activity as the main effector of stathmin in the control of adhesion-dependent MT polymerization and of cell movement. This is in agreement with previous observations suggesting that the catastrophe-promoting N-terminal domain plays a more prominent role in controlling the spindle formation during mitosis (Holmfeldt *et al.*, 2001).

We demonstrated that stathmin is phosphorylated after cell adhesion to ECM on at least three different serine residues, suggesting that adhesion to ECM contributes to the regulation of stathmin activity through the modification of its phosphorylation status. The finding that stathmin^{Q18E}, unable to undergo S16 phosphorylation, displays a gain of function in stimulating sarcoma cell motility suggests that S16 phosphorylation could represent an important event in the regulation of cell motility by stathmin. Accordingly, recent data demonstrated that stathmin is phosphorylated on S16 in developing neurons adherent to laminin and that this phosphorylation is necessary for proper neuritis outgrowth (Watabe-Uchida *et al.*, 2006). The role of adhesion-dependent S25 and S38 phosphorylations in cell motility remains less clear, because both these residues are readily phosphorylated in the stathmin^{Q18E} protein. On the contrary, stathmin^{Q18E} did not stimulate HT-1080 cells growth.

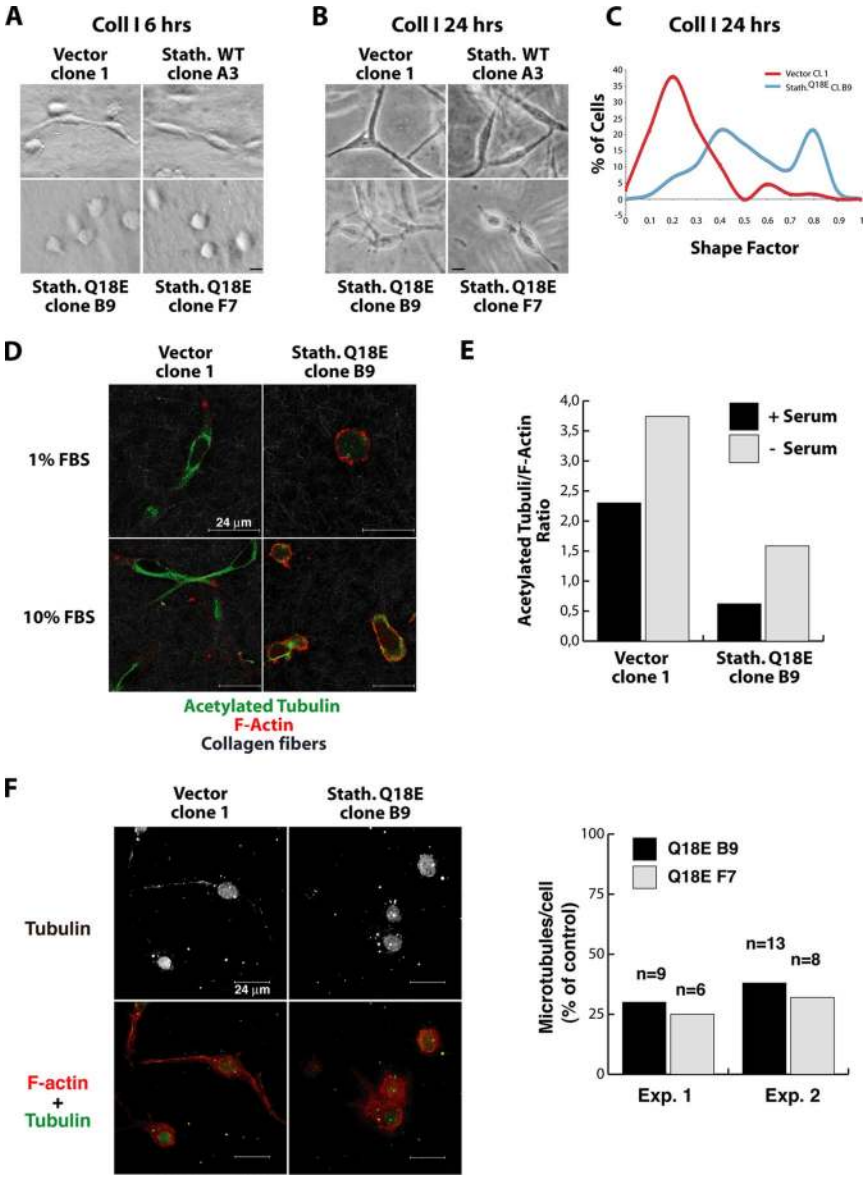

Figure 7. Stathmin^{Q18E} expression alters HT-1080 cell morphology in 3D matrices. (A) Hoffman microscopy images of HT-1080 cell clones included in 3D Coll I and cultured in serum-reduced (1% FBS) medium for 6 h. Bar, 30 μm. (B) Phase-contrast microscopy images of HT-1080 cell clones immersed in 3D Coll I and cultured in serum-reduced medium for 24 h. Bar, 30 μm. (C) Assessment of the "Shape Factor" of HT-1080 V1 and stathmin^{Q18E} B9 clones included in 3D Coll I and cultured in serum-reduced medium for 24 h. The Shape Factor was calculated using the formula $4\pi A/P^2$. (D) Confocal microscopy analysis of HT-1080 cell clones vector 1 and stathmin^{Q18E} B9 immersed in Coll I, cultured in the indicated media (1% FBS or 10% FBS) for 24 h and stained for acetylated tubulin (green) and F-actin (red). Collagen fibers were visualized in gray using the Laser 488 reflection. (E) Quantification of the mean fluorescence intensity of acetylated tubulin and F-actin, expressed as the acetylated tubulin/F-actin ratio. Data represent the means of at least 50 cells for each condition, analyzed by confocal microscopy coupled with computer software analysis ($p < 0.001$ of V1 vs. B9 cells, using Student's t test). (F) Typical images of HT-1080 V1 and stathmin^{Q18E} B9 cell clones included in 3D Coll I and subjected to the tubulin dilution assay and stained with anti α-tubulin FITC-conjugated Ab and AlexaFluor543-phalloidin. Tubulin staining is shown in gray in the top panels and in green in the bottom panels. Phalloidin staining is in red. The graph shows the quantification of detectable MTs per cell in stathmin^{Q18E}-expressing cells in two independent experiments. Data are expressed as percent of MT number with respect to control cells; n represents the number of analyzed cells.

This observation is in line with the work of Misek *et al.* (2002) that showed minor effects on normal fibroblasts growth in 2D assays after expression of ectopic stathmin^{Q18E} protein. These authors showed indeed that stathmin^{Q18E} had transforming properties and increased cell growth in soft agar assay, an effect that could not be appreciated in our model because we used the already transformed HT-1080 cells.

Importantly, our results demonstrate that stathmin is able to promote sarcoma cell motility through or within the ECM in vitro and stimulate local invasion and/or metastasis formation in vivo. These activities are associated with a change in cell morphology and a decrease in stable MT content, when cells are included in a 3D matrix or grown in vivo. Both cytoskeletal dynamics and cell shape dictate migration mode and efficiency in a 3D context (Friedl and Wolf, 2003; Sahai and Marshall, 2003; Wolf *et al.*, 2003). It has been proposed that motility of rounded cells is characterized by reduced cell elongation, relatively weak cell–matrix interactions, and the ability of the cells to squeeze their body to pass through the ECM fibers, using small ruffles or bleb-like propulsive translocation. This mode of cellular migration has been defined as "amoeboid" motility (Friedl and Wolf, 2003; Sahai and Marshall, 2003; Wolf *et al.*, 2003). It is then conceivable that a more dynamic and flexible MT network (due to increased stathmin activity) could cause a switch in the migration mode, inducing an "amoeboid"-like motility both in vitro and in vivo. This might not only promote tumor cell evasion from the primary site but also result in a more rapid and distant dissemination, as proposed also by others (Friedl and Wolf, 2003). The importance of assaying cell flexibility in response to increased microtubule turnover in a 3D context is underscored by the observation that overexpression of stathmin^{WT} or stathmin^{Q18E} did not increase cell motility in 2D assays (Figure 5 and Ng *et al.*, 2006). It is important to note that the behavior of control and stathmin-overexpressing clones in random motility substantially differs when 2D versus 3D conditions are analyzed. This allows us to hypothesize that 3D signaling from the matrix is specifically relevant for the enhancement of motility induced by stathmin. Our data suggest that phosphorylation of stathmin after cell adhesion to the ECM could contribute at least in part to the stabilization of the MT

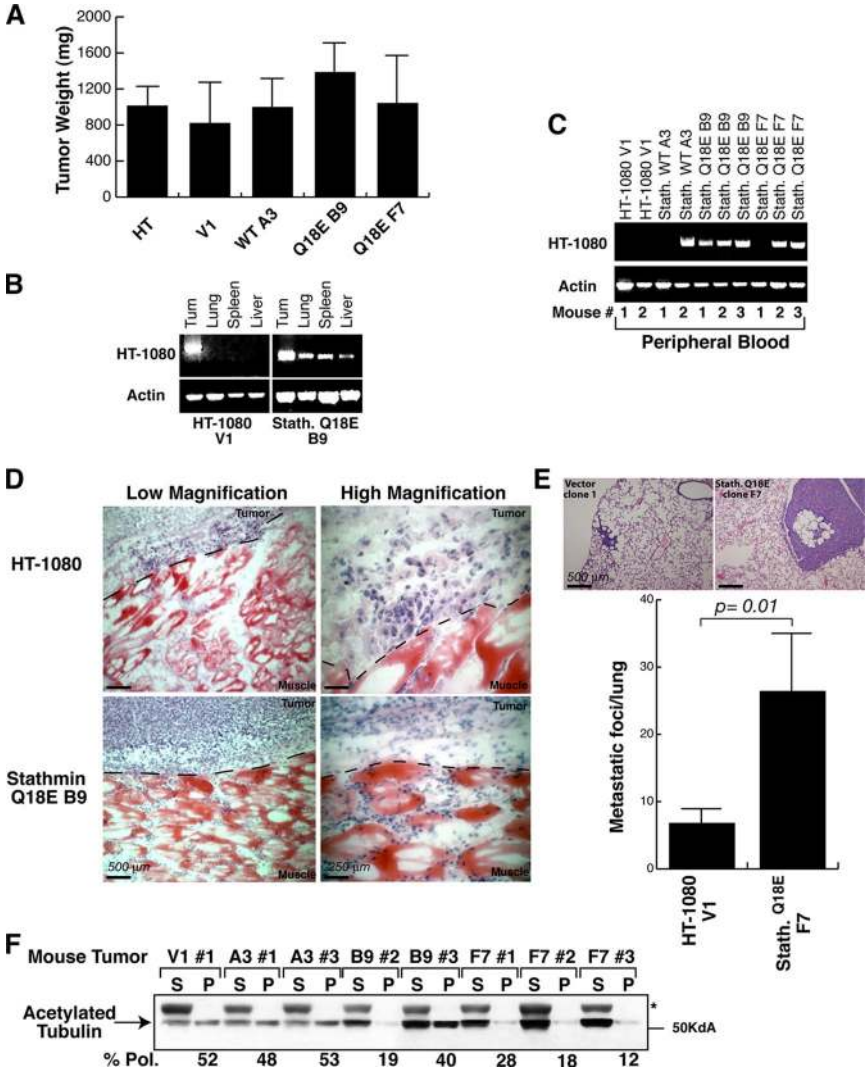

Figure 8. Stathmin expression enhances HT-1080 cell invasion and metastasis formation in vivo. (A) In vivo growth of parental and stably transfected HT-1080 cell clones subcutaneously injected in nude mice. (B) RT-PCR analysis of RNA of tissues explanted from mice injected with HT-1080 V1 and stathmin^{Q18E} B9 cell clones. Amplification was performed using primers designed on the transfected vectors. Amplification of actin was used as a control. (C) RT-PCR analysis of RNA extracted from blood derived from mice subcutaneously injected with HT-1080 cell clones, using primers designed on the transfected vectors. Amplification of actin was used as a control. (D) Local invasion of HT-1080 cells included in Matrigel and then injected subcutaneously into nude mice (n = 4). Fifteen days after the injection, tumors were explanted and analyzed by H&E staining. Typical images acquired at 10× (left panels) or 40× (right panels) are shown. (E) Lung metastasis formation in mice injected in the tail vein with HT-1080 V1 or stathmin^{Q18E} F7 cell clones and analyzed by H&E staining 30 d after the injection. The quantification of lung metastases in mice injected with HT-1080 V1 or stathmin^{Q18E} F7 cell clones is shown in the graph. (F) Analysis of soluble and polymerized acetylated tubulin content in tumors derived from the indicated HT-1080 cell clones. Percentage of polymerized fractions (% Pol.) of acetylated tubulin was calculated as described above.

network and that impairing this pathway may result in a switch versus an amoeboid type of motility. Our data also confirm that the physicochemical requirements in the cell for 2D and 3D migration are distinct. A clarifying example is given by the studies of Marshall and colleagues, on the role of the small GTPase RhoA in cell motility. These authors demonstrated that hyperactive RhoA decreases wound-healing motility (Vial *et al.*, 2003) but increases or does not affect (depending on the cell type) cell invasion in a 3D context (Sahai and Marshall, 2003). Moreover, recent data suggest that increased RhoA activity at the cell periphery by Smurf1-silencing results in decreased 2D motility, but increased 3D invasive potential, in different tumor cell types (Sahai *et al.*, 2007). These data further confirm that the ability of cells to move on a 2D substrata does not always parallel the invasiveness of cancer cells. Interestingly, increasing evidence underscores the existence of a tight relationship between MT dynamics and small GTPase activity, because MT stability can regulate GTPase activity (Xu *et al.*, 2005) and, in turn, small GTPases can affect adhesion-dependent MT stabilization (Palazzo *et al.*, 2004), at least in part acting on stathmin (Watabe-Uchida *et al.*, 2006).

It is interesting to note that stathmin down-regulation in vivo in mice and *Drosophila* results in decreased motility of proliferating neurons (Jin *et al.*, 2004) and germ and border cells (Ozon *et al.*, 2002; Borghese *et al.*, 2006), strongly supporting a promigratory role for this protein. Moreover, the fact that the MT-stabilizing protein MAP2 is down-regulated in metastatic melanomas with respect to primary tumors (Soltani *et al.*, 2005)—whereas stathmin is overexpressed in metastatic versus clinically localized prostate carcinomas (Varambally *et al.*, 2005), invasive recurrent hepatocarcinomas (Yuan *et al.*, 2006), advanced mammary carcinomas (Van't Veer *et al.*, 2002), and recurrent/metastatic sarcomas (our work)—suggests that decreased MT stability could be a general feature in the process of metastasis formation. Our findings indicate that increased stathmin expression and/or activity stimulates sarcoma cell migration in vitro, enhances local and distant dissemination in mice, and correlates with sarcoma recurrence and metastasis formation in human disease. Altogether, these data strongly point to stathmin as a potential prognostic factor and a promising target for biological therapies in refractory diseases, at least in soft tissue sarcomas.

ACKNOWLEDGMENTS

We are grateful to Dr. André Sobel (INSERM, Paris, France) for providing the anti-phospho-stathmin antibodies and to Dr. Greg G. Gundersen (Columbia University, New York, NY) for providing the anti-Glu-Tubulin Ab. We thank

Bruna Wassermann and Margit Ott for excellent technical support. This work was supported by grants from Associazione Italiana Ricerca sul Cancro (AIRC) and partially from Association for International Cancer Research (AICR) and Ministero della Salute to G.B. F.L. is recipient of an AIRC fellowship.

REFERENCES

Baldassarre, G., Belletti, B., Nicoloso, M. S., Schiappacassi, M., Vecchione, A., Spessotto, P., Morrione, A., Canzonieri, V., and Colombatti, A. (2005). p27(Kip1)-stathmin interaction influences sarcoma cell migration and invasion. Cancer Cell *7*, 51–63.

Belmont, L. D., and Mitchison, T. J. (1996). Identification of a protein that interacts with tubulin dimers and increases the catastrophe rate of microtubules. Cell *84*, 623–631.

Borghese, L., Fletcher, G., Mathieu, J., Atzberger, A., Eades, W. C., Cagan, R. L., and Rorth, P. (2006). Systematic analysis of the transcriptional switch inducing migration of border cells. Dev. Cell *10*, 497–508.

Curmi, P. A., Gavet, O., Charbaut, E., Ozon, S., Lachkar-Colmerauer, S., Manceau, V., Siavoshian, S., Maucuer, A., and Sobel, A. (1999). Stathmin and its phosphoprotein family: general properties, biochemical and functional interaction with tubulin. Cell Struct. Funct. *24*, 345–357.

Curmi, P. A., Nogues, C., Lachkar, S., Carelle, N., Gonthier, M. P., Sobel, A., Lidereau, R., and Bieche, I. (2000). Overexpression of stathmin in breast carcinomas points out to highly proliferative tumours. Br. J. Cancer *82*, 142–150.

Etienne-Manneville, S. (2004). Actin and microtubules in cell motility: which one is in control? Traffic *5*, 470–477.

Friedl, P., and Brocker, E. B. (2000). The biology of cell locomotion within three-dimensional extracellular matrix. Cell. Mol. Life Sci. *57*, 41–64.

Friedl, P., and Wolf, K. (2003). Tumour-cell invasion and migration: diversity and escape mechanisms. Nat. Rev. Cancer *3*, 362–374.

Gavet, O., Ozon, S., Manceau, V., Lawler, S., Curmi, P., and Sobel, A. (1998). The stathmin phosphoprotein family: intracellular localization and effects on the microtubule network. J. Cell Sci. *111*(Pt 22), 3333–3346.

Giampietro, C., Luzzati, F., Gambarotta, G., Giacobini, P., Boda, E., Fasolo, A., and Perroteau, I. (2005). Stathmin expression modulates migratory properties of GN-11 neurons in vitro. Endocrinology *146*, 1825–1834.

Holmfeldt, P., Larsson, N., Segerman, B., Howell, B., Morabito, J., Cassimeris, L., and Gullberg, M. (2001). The catastrophe-promoting activity of ectopic Op18/stathmin is required for disruption of mitotic spindles but not interphase microtubules. Mol. Biol. Cell *12*, 73–83.

Howell, B., Larsson, N., Gullberg, M., and Cassimeris, L. (1999). Dissociation of tubulin-sequestering and microtubules catastrophe-promoting activities of Oncoprotein 18/stathmin. Mol. Biol. Cell *10*, 105–118.

Jin, K. *et al.* (2004). Proteomic and immunochemical characterization of a role for stathmin in adult neurogenesis. FASEB J. *18*, 287–299.

Khawaja, S., Gundersen, G. G., and Bulinski, J. C. (1988). Enhanced stability of microtubules enriched in detyrosinated tubulin is not a direct function of detyrosination level. J. Cell Biol. *106*, 141–149.

Koppel, J., Boutterin, M. C,. Doye, V., Peyro-Saint-Paul, H., and Sobel, A. (1990). Developmental tissue expression and phylogenetic conservation of stathmin, a phosphoprotein associated with cell regulations. J. Biol. Chem. *265*, 3703–3707.

Liao, G., Nagasaki, T., and Gundersen, G. G. (1995). Low concentrations of nocodazole interfere with fibroblast locomotion without significantly affecting microtubule level: implications for the role of dynamic microtubules in cell locomotion. J. Cell Sci. *108*, 3473–3483.

Melhem, R. F., Zhu, X. X., Hailat, N., Strahler, J. R., and Hanash, S. M. (1991). Characterization of the gene for a proliferation-related phosphoprotein (oncoprotein 18) expressed in high amounts in acute leukemia. J. Biol. Chem. *266*, 17747–17753.

Misek, D. E., Chang, C. L., Kuick, R., Hinderer, R., Giordano, T. J., Beer, D. G., and Hanash, S. M. (2002). Transforming properties of a Q18→E mutation of the microtubule regulator Op18. Cancer Cell *2*, 217–228.

Ng, D.C.H., Lin, B. H., Lim, C. P., Huang, G., Zhang, T., Poli, V., and Cao, X. (2006). Stat3 regulates microtubules by antagonizing the depolymerization activity of stathmin. J. Cell Biol. *172*, 245–257.

Ozon, S., Guichet, A., Gavet, O., Roth, S., and Sobel, A. (2002). *Drosophila* stathmin: a microtubule-destabilizing factor involved in nervous system formation. Mol. Biol. Cell *13*, 698–710.

Palazzo, A. F., Eng, C. H., Schlaepfer, D. D., Marcantonio, E. E., Gundersen, G. G. (2004). Localized stabilization of microtubules by integrin- and FAK-facilitated Rho signaling. Science *303*, 836–839.

Peris, L. *et al.* (2006). Tubulin tyrosination is a major factor affecting the recruitment of CAP-Gly proteins at microtubule plus ends. J. Cell Biol. *174*, 839–849.

Price, D. K., Ball, J. R., Bahrani-Mostafavi, Z., Vachris, J. C., Kaufman, J. S., Naumann, R. W., Higgins, R. V., and Hall, J. B. (2000). The phosphoprotein Op18/stathmin is differentially expressed in ovarian cancer. Cancer Invest. *18*, 722–730.

Rodriguez, O. C., Schaefer, A. W., Mandato, C. A., Forscher, P., Bement, W. M., and Waterman-Storer, C. M. (2003). Conserved microtubule-actin interactions in cell movement and morphogenesis. Nat. Cell Biol. *5*, 599–609.

Sahai, E., and Marshall, C. J. (2003). Differing modes of tumour cell invasion have distinct requirements for Rho/ROCK signalling and extracellular proteolysis. Nat. Cell. Biol. *5*, 711–719.

Sahai, E., Garcia-Medina, R., Pouyssegur, J., and Vial, E. (2007). Smurf1 regulates tumor cell plasticity and motility through degradation of RhoA leading to localized inhibition of contractility J. Cell Biol. *176*, 35–42.

Small, J. V., Geiger, B., Kaverina, I., and Bershadsky, A. (2002). How do microtubules guide migrating cells? Nat. Rev. Mol. Cell Biol. *3*, 957–964.

Sobel, A., Boutterin, M. C., Beretta, L., Chneiweiss, H., Doye, V., and Peyro-Saint-Paul, H. (1989). Intracellular substrates for extracellular signaling. Characterization of a ubiquitous, neuron-enriched phosphoprotein (stathmin). J. Biol. Chem. *264*, 3765–3772.

Soltani, M. H., Pichardo, R., Song, Z., Sangha, N., Camacho, F., Satyamoorthy, K., Sangueza, O. P., and Setaluri, V. (2005). Microtubule-associated protein 2, a marker of neuronal differentiation, induces mitotic defects, inhibits growth of melanoma cells, and predicts metastatic potential of cutaneous melanoma. Am. J. Pathol. *166*, 1841–1850.

Van 't Veer, L. J. *et al.* (2002). Gene expression profiling predicts clinical outcome of breast cancer. Nature *415*, 530–536.

Varambally, S. *et al.* (2005). Integrative genomic and proteomic analysis of prostate cancer reveals signatures of metastatic progression. Cancer Cell *8*, 393–406.

Vial, E., Sahai, E., and Marshall, C. J. (2003). ERK-MAPK signaling coordinately regulates Rac1 and RhoA for tumor cell motility. Cancer Cell *4*, 67–79.

Watabe-Uchida, M., John, K. A., Janas, J. A., Newey, S. E., and Van Aelst, L. (2006). The Rac activator DOCK7 regulates neuronal polarity through local phosphorylation of stathmin/Op18. Neuron *51*, 727–739.

Verhey, K. J., and Gaertig, J. (2007). The tubulin code. Cell Cycle *6*, 2152–2160.

Wittmann, T., Bokoch, G. M., and Waterman-Storer, C. M. (2004). Regulation of microtubule destabilizing activity of Op18/stathmin downstream of Rac1. J. Biol. Chem. *279*, 6196–6203.

Wolf, K., Mazo, I., Leung, H., Engelke, K., von Andrian, U. H., Deryugina, E. I., Strongin, A. Y., Brocker, E. B., and Friedl, P. (2003). Compensation mechanism in tumor cell migration: mesenchymal-amoeboid transition after blocking of pericellular proteolysis. J. Cell Biol. *160*, 267–277.

Yuan, R. H., Jeng, Y. M., Chen, H. L., Lai, P. L., Pan, H. W., Hsieh, F. J., Lin, C. Y., Lee, P. H., and Hsu, H. C. (2006). Stathmin overexpression cooperates with p53 mutation and osteopontin overexpression, and is associated with tumour progression, early recurrence, and poor prognosis in hepatocellular carcinoma. J. Pathol. *209*, 549–558.

Xu, J., Wang, F., Van Keymeulen, A., Rentel, M., and Bourne, H. R. (2005). Neutrophil microtubules suppress polarity and enhance directional migration. Proc. Natl. Acad. Sci. USA *102*, 6884–6889.